# Subwavelength Radio Repeater System Utilizing Miniaturized Antennas and Metamaterial Channel Isolator

Kamal Sarabandi, *Fellow, IEEE*, and Young Jun Song, *Student Member, IEEE*

***Abstract*—Implementation of a novel high gain miniaturized radio repeater for improving wireless network connectivity in complex environment is presented in this paper. Unlike existing repeater systems, this system utilizes two closely spaced low profile miniaturized planar antennas capable of producing omnidirectional and vertical radiation pattern as well as a channel isolator layer that serves to decouple the adjacent antennas. The metamaterial based channel isolator serves as an electromagnetic shield, thus enabling it to be built in a sub-wavelength size of $0.07\lambda_0^2 \times 0.014\lambda_0$, the smallest repeater ever built. A prototype of the small radio repeater is fabricated to verify the design performance through a standard free-space measurement setup. The feasibility of amplifying and re-transmitting the received signal is demonstrated through measurement which compares well with the numerical simulation results.**

***Index Terms*—Antenna array mutual coupling, electromagnetic shielding, indoor radio communication, multiaccess communication.**

## I. Introduction

### A. Background of This Study

FOR wireless network systems, the path-loss between the transmitter and receiver is a critical factor that determines the possible range of communication between two nodes. Complex environments such as urban canyons and building interiors often contain numerous obstacles that impede the line-of-sight (LOS) communication and increase the path-loss. The existing long range ad-hoc communication network relies on multipath (multiple reflection, diffraction, and penetration through obstacles). In these environments especially at high frequencies the path-loss dramatically increases, which often requires higher transmitter power and closely spaced communication nodes. Furthermore, as transmitter power increases or as transmitting nodes become closer, the potential for mutual interference between communication cells increases which, if present, can cause degradation in coverage capacity. Additionally, a topology that uses closely spaced nodes will be more expensive than a similar topology sparsely populated with nodes. To overcome these situations and to help improve the ground area coverage of communication signals without increasing the transmitter power, radio repeaters have been extensively used in various application scenarios. Numerous studies regarding feasibility and operation of the radio repeater have been presented in [1]–[4].

Additionally, numerous commercial products utilizing the concept of the radio repeater have been introduced and fabricated such as in [5] and [6]. The main objective of the radio repeater in these scenarios is to achieve enhanced connectivity by amplifying a radio signal through an active device as shown in Fig. 1. For the downlink communication, from a base station to an end-node/unit, the signal originating at the base station is linked through the Receive antenna (RX) of repeater, amplified, and retransmitted through the Transmit antenna (TX), and vice versa for the uplink direction. However, the mutual coupling between a repeater's RX and TX antennas generates a positive feedback loop as shown in Fig. 1. When the gain of the RF amplifier is greater than the isolation level of the RX and TX antennas, the overall system will start to oscillate, and the communication coverage of that micro cell cannot be established. Thus, the level of mutual coupling limits the performance of a radio repeater as well as the dimension and cost of the overall system. To circumvent this intrinsic problem, generally two approaches have been proposed. The first method is to divide the frequencies of the uplink and downlink signals. This methodology utilizes a frequency division duplex (FDD) to reduce the mutual coupling by separating signal frequencies. However, it requires complex circuitry, larger size, and a common protocol to manage frequency allocation, which all imply higher cost and much more power consumption. The second method is to adapt a time division duplex (TDD) in time domain. This also introduces additional logic circuitry, latency, and knowledge of the repeater, transmitter and receiver locations, as presented in [7] and [8].

In this paper, a new device is proposed to overcome the adverse effect of various complex environments by reducing the path-loss. To enhance radio connectivity and maintain low-power communication, a very small radio repeater with a large radar cross section (RCS) and an omnidirectional radiation pattern is proposed. The proposed radio repeater receives the LOS signal from the transmitter, amplifies it, and then retransmits the amplified signal omnidirectionally, which establishes a secondary LOS to arbitrary receivers. Thus, a

Manuscript received January 13, 2010; revised November 04, 2010; accepted December 10, 2010. Date of publication May 10, 2011; date of current version July 07, 2011. This research was supported by the U.S. Army Research Laboratory under contract W911NF and prepared through collaborative participation in the Microelectronics Center of Micro Autonomous Systems and Technology (MAST) Collaborative Technology Alliance (CTA).

The authors are with the Radiation Laboratory, Department of Electrical Engineering and Computer Science, The University of Michigan at Ann Arbor, Ann Arbor, MI 48109-2122 USA (e-mail: saraband@eecs.umich.edu; yjsong@umich.edu).

Color versions of one or more of the figures in this paper are available online at http://ieeexplore.ieee.org.

Digital Object Identifier 10.1109/TAP.2011.2152320

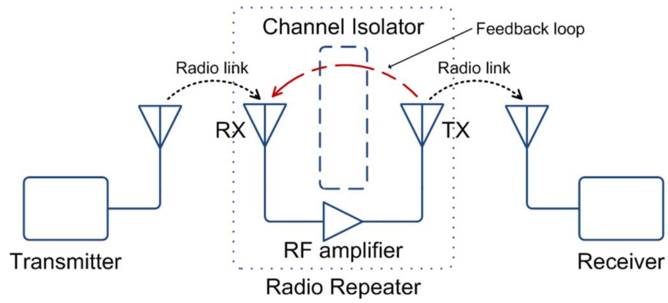


Fig. 1. Schematic of radio link using radio repeater.

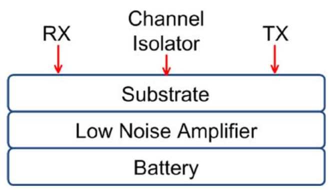


Fig. 2. Schematic of proposed small radio repeater.

series of small radio repeaters can enhance radio connectivity by establishing a LOS with the repeater nodes.

### B. Benefits of the Proposed Small Radio Repeater

Fig. 2 shows the proposed Small Radio Repeater. It consists of two miniaturized planar antennas capable of supporting an omnidirectional pattern and vertical polarization. Additionally, a metamaterial based isolator structure is used, and active RF amplification circuitry as well as a battery is integrated into the radio repeater platform. Since RX/TX of the proposed repeater shows omnidirectionality over the H plane, the uplink and downlink signal paths can be established through a single circuit path. This can reduce complexity and power consumption of RF circuitry. In addition, pure vertical polarization allows for a simple antenna structure for the base station and end-node/units as well as a decreased path-loss along the channel. It is well understood that for near-earth wave propagation scenarios vertically polarized waves experience much less path-loss compared to horizontally polarized waves as presented in [9]. To achieve the compact dimension of the radio repeater, a metamaterial based channel isolator is utilized. By generating the normal magnetic field along the signal path between RX and TX, artificial magnetic walls are generated that serve to suppress the electromagnetic wave propagation from RX to TX antennas.

The proposed radio repeater occupies a very small area $(0.07\lambda_0^2)$ with a very short height $(\lambda_0/70)$ without its active circuitry. The passive components such as two miniaturized antennas and metamaterial based isolator are presented and verified in this paper. The prototype is fabricated using a commercially available dielectric substrate. In addition, a commercially available RF amplifier and battery are used to verify the operational feasibility of the proposed repeater. This configuration is shown to boost the power level of the received signal by 32 dB.

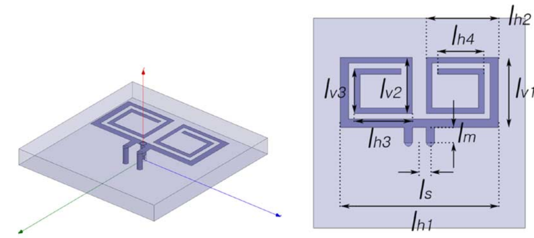


(a) (b)

Fig. 3. Modified MMA: (a) topology of modified MMA for small radio repeater; (b) design parameters.

TABLE I
DESIGNED PARAMETERS OF MODIFIED MMA

| $l_{h1}$ | $l_{h2}$ | $l_{h3}$ | $l_{h4}$ | $l_{v1}$ | $l_{v2}$ |
|---|---|---|---|---|---|
| 11.20mm | 5.10mm | 4.10mm | 3.30mm | 5.00mm | 4.00mm |

| $l_{v3}$ | $l_m$ | $l_s$ |
|---|---|---|
| 3.20mm | 1.10mm | 0.78mm |

## II. DESIGN SPECIFICATIONS

### A. Miniaturized Repeater Antenna

According to antenna theory, the intensity and polarization of the radiated field are proportional to the level and direction of the current distribution over the antenna. In many practical miniaturized antennas, the level of the excited current is limited by the impedance mismatch between the feeding network and the antenna itself. To achieve a low-profile miniaturized antenna, a quarter-wave microstrip resonator fed near the short-circuited end is used. To achieve miniaturization and impedance matching a four-arm spiral shape quarter-wave resonator structure was utilized and presented in [10]. Although a good input reflection coefficient at the frequency of operation can be obtained, this antenna requires two layers; an upper layer consisting of the open-ended spiral shape line and a lower layer consisting of the short-circuited transmission line for the matching network to radiate the power effectively. This physical structure increases complexity and cost for fabrication. And any misalignment between the two layers can shift the operation frequency.

The proposed new approach is to place the matching network at the same layer of the miniaturized antenna as shown in Fig. 3. Although the main radiation is from the shorted pins, some radiation is emanated from the spiral arms. The polarization of the radiated field from the spiral arms is horizontal. Therefore, each of the spiral arms should be placed in a symmetrical manner in order to minimize horizontally polarized radiated field. Symmetry of these arms is essential to cancel such radiated fields and eventually achieve an omnidirectional vertically polarized radiation pattern. In addition, symmetry and close spacing $(1.56\ \mathrm{mm} \approx \lambda_0/70)$ of the shorting pins enable the excited currents through these pins to be in-phase. The short circuited currents that pass through the four vertical pins are the dominant radiating elements and responsible for the vertically polarized radiated field. The optimized miniaturized multi-elements monopole antenna (MMA) is designed using a commercial finite element method solver (Ansoft's HFSS ver. 11.1).

To be incorporated into the small radio repeater, the optimized MMA must be further modified to achieve smaller dimensions. Because of the sub-wavelength dimension of the proposed radio

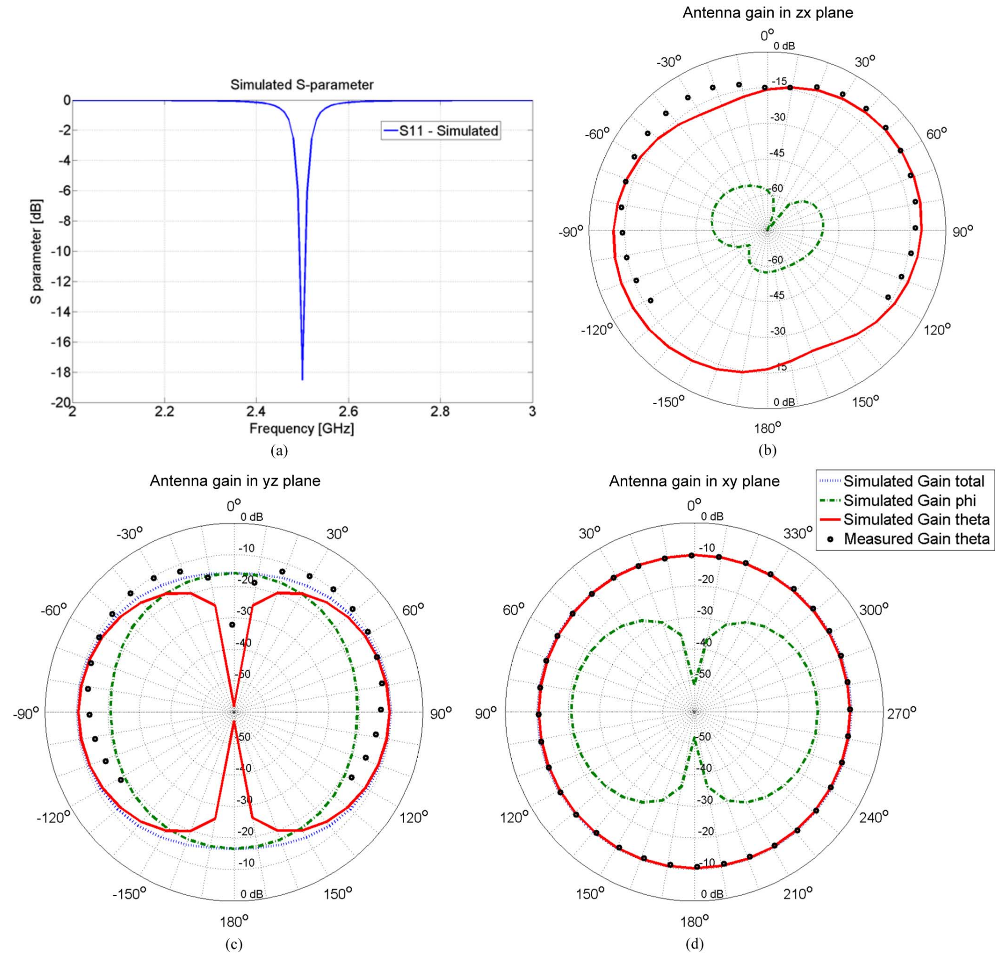


Fig. 4. Simulated responses of modified MMA: (a) $S_{11}$ response; (b) radiation pattern in E(zx) plane; (c) radiation pattern in E(yz) plane; (d) radiation pattern in H(xy) plane.

repeater, a pair of the optimized MMA with four arms can produce a high level of mutual coupling within the small ground plane. Thus, the objective is to modify the MMA geometry so that mutual coupling can be reduced while maintaining the polarization purity and the desired radiation pattern. By utilizing only two arms of the MMA with a symmetric topology as shown in Fig. 3, the horizontal current cancellation and reduction of mutual coupling can be achieved at the expense of an asymmetric radiation pattern in the E plane. The modified MMA is designed and verified using Ansoft's HFSS. The designed topology and parameters are shown in Fig. 3. The physical dimensions are optimized for operation around 2.5 GHz and summarized in Table I. And all line length and spacing (between traces) values are set to 0.4 mm, except for $l_{h1}$, $l_{v1}$ and $l_m$ which are set to 0.6 mm. Fig. 4(a) presents the simulated input reflection coefficient of the modified MMA. As can be seen, the modified MMA shows a $-18.5$ dB of input reflection coefficient at the design frequency. The radiation pattern of the modified MMA is shown in Fig. 4(b), (c), and (d). The vertical polarization in the H-plane shows an omnidirectional pattern, similar to that of a monopole. In addition, the level of the horizontal polarization in the H-plane is negligible compared to the vertical polarization, which implies that the cancellation between horizontal electric current is achieved effectively. Furthermore, the transmission line based antenna can be fabricated using the standard printed circuit technology. This serves to reduce the alignment error observed in the multi-layer design, and hence the fabrication process and the discrepancy between the simulation and measurement are reduced significantly.

### B. Metamaterial Based Channel Isolator

In practical antenna systems, the mutual coupling between adjacent antennas restricts compact integration of multiple antennas in a small area for applications such as multiple input and multiple output (MIMO) communication systems. To suppress the mutual coupling, various approaches have been studied and presented in [11]–[13]. In general, these studies can be categorized into two approaches. The first method is to engineer the electric and magnetic properties of the material, such as the permittivity and permeability, by introducing an artificial structure. For example, a mushroom-like structure can suppress the mutual coupling by introducing a negative refractive index, as shown in [11] and [12]. Another method utilizes metamaterial insulators to block the EM energy from being transmitted across the insulation boundary, as shown in [13]. This metamaterial insulator consists of magneto-dielectric embedded circuits, which can be modeled as parallel LC resonant circuits. However, both approaches have intrinsic limitations when attempting to suppress the mutual coupling of antennas at the commercial ISM

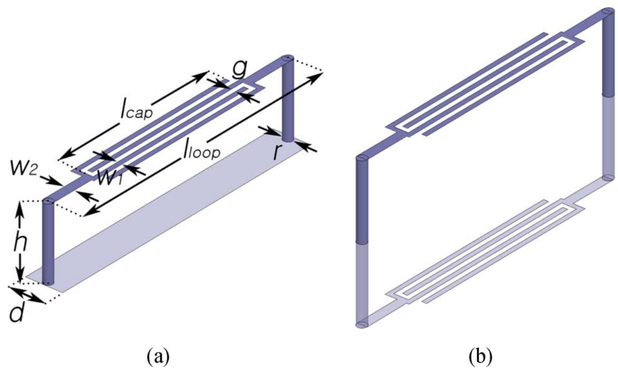


Fig. 5. Unit cell of channel isolator: (a) topology of unit cell; (b) square loop by image theory.

frequency band (around 2.5 GHz). The artificial structure requires large physical dimensions, and the metamaterial insulator causes fabrication complexity and cost.

To address these limitations, a metamaterial based channel isolator is proposed and designed as shown in Fig. 5(a). The proposed isolator is designed to resonate at the desired channel frequency and decrease the mutual coupling by suppression of the surface waves in the substrate generated by the vertical pins of the MMA. The vertical pins create a transverse magnetic (TM) wave in the substrate with zero cutoff frequency. The magnetic field is parallel to the ground plane and perpendicular to the pins. To inhibit propagation of the TM surface wave, an electromagnetic band-gap (EBG) metamaterial layer can be utilized. The advantage of the band-gap material is that it creates an equivalent open circuit to the surface wave as opposed to a short-circuit that a metallic wall can produce.

The band-gap metamaterial consists of an array of the parallel LC resonant circuits that are magnetically coupled with the substrate mode. This is realized using unit cells that consist of vertical wires and horizontal conducting strips, which behave like a distributed inductor and a distributed capacitor, respectively. Using image theory, when each loop is imaged a larger loop having a larger inductance and a smaller capacitance is formed as shown in Fig. 5(b). Assuming the fundamental mode propagates from the TX to the RX through the substrate, the horizontally polarized magnetic field linked by the square loop induces an electric current on the vertical wires. In addition, this induced current generates a magnetic field which is perpendicular to the loop. When the unit cells are closely spaced to each other, the inductance of the loops is increased and the periodic array acts like a solenoid. At resonance the periodic layer acts as a perfect magnetic conductor (PMC) plane. Due to the mutual coupling of the adjacent loops, the self inductance of the square loop as shown in Fig. 5(b) can be obtained from [14]

$$L_s = \frac{\mu_r \mu_0 A_{loop}}{d} \tag{1}$$

where $A_{loop} = h l_{loop}$ is the internal area of the loop and $d$ is the periodicity of unit cells.

The quality factor (Q) of the equivalent single pole isolator affects the performance and isolation bandwidth. Thus, commercial lumped capacitors with finite deviation of capacitance values and low Q factor will cause the suppression of the mutual coupling to deteriorate. To simultaneously reduce the deviation of these values, improve the Q factor, and lower the cost of fabrication, printed circuit technology can be utilized to implement the capacitors. As mentioned, the magnetic field induces the electric current on the vertical wires, and this current transforms to a displacement current (electric field) as it gets through the gaps between the fingers of the series interdigital capacitor. As most of the electric field between the metallic strips of this capacitor is in the gap and perpendicular to the metallic edges, its capacitance can be computed from the capacitance per unit length of two thin co-planar strips given by [15]

TABLE II
DESIGNED PARAMETERS OF CHANNEL ISOLATOR

| $l_{loop}$ | $l_{cap}$ | $g$ | $w_1$ | $w_2$ |
|---|---|---|---|---|
| 6.25mm | 3.84mm | 0.10mm | 0.10mm | 0.20mm |

| $h$ | $d$ | $r$ | $n$ |
|---|---|---|---|
| 1.57mm | 0.81mm | 0.20mm | 4 |

$$C_{i,e} = \epsilon_r \epsilon_0 \frac{K(k_{i,e})}{K\left(\sqrt{1 - {k_{i,e}}^2}\right)} \tag{2}$$

$$k_i = sin\left(\frac{\pi}{2}\eta\right) \quad \text{and} \quad k_e = 2\frac{\sqrt{\eta}}{1+\eta} \tag{3}$$

where $\eta = w_1/(w_1 + g)$ is the metallization ratio and $K(k)$ is the complete elliptic integral of first kind defined by

$$K(k) = \int_0^{\pi/2} \frac{d\phi}{\sqrt{1 - k^2 \sin^2 \phi}}. \tag{4}$$

Since the individual capacitors between fingers are connected in parallel, the total capacitance per unit length of interdigital capacitor is equal to

$$C = (n-3)\frac{C_i}{2} + 2\frac{C_i C_e}{C_i + C_e} \quad \text{for} \quad n > 3 \tag{5}$$

where $C_i$ is the capacitance between inner strips, $C_e$ is between outer and inner strips, and $n$ is the number of fingers. Hence, the total capacitance of the proposed isolator can be calculated easily from $C_s = C l_{cap}$, where $l_{cap}$ is the length of the fingers. The interdigital capacitor is centered between two vertical wires. The designed parameters are summarized in Table II. The length and height of the unit cell are chosen to be 6.25 mm × 1.57 mm. The corresponding inductance and capacitance of the unit cell are thus found to be 15.2132 nH and 0.1869 pF, respectively. Based on this calculation, the self resonant frequency is calculated to be 2.98 GHz.

## III. PARAMETRIC STUDIES AND OPTIMIZATION

### A. Optimal Configuration Without the Isolator

In Section II, the principle of operation of the MMA was established. The modified MMA with two symmetric arms and vertical pins was designed on a small ground plane and was

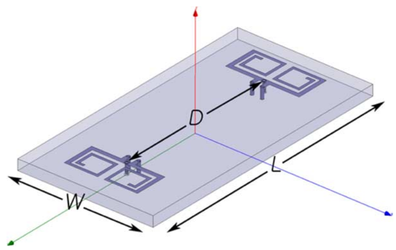


Fig. 6. Repeater platform without channel isolator.

shown to produce a very good impedance match and vertical polarization. This design is further optimized to be integrated into the channel isolator as shown in Fig. 6. As mentioned before, two arms of the original MMAs that would come close to the metamaterial isolator are removed. The magnetic field from these arms could have coupled to the isolator loops and established a link between the two antennas instead of isolating them. In a miniaturized antenna, the size of the ground plane can also affect the performance of the antenna. The edge currents on the ground plane affect the radiation pattern, directivity, and polarization. To maintain small physical dimensions, the design parameters for the optimized configuration include the position of the TX and RX antennas as well as the dimensions of the ground plane. The optimization is performed using HFSS to achieve impedance matching at the desired frequency, maintaining an isolation level smaller than −20 dB, and minimizing the size of the ground plane.

Fig. 7(a) represents a parametric study where the simulation responses of $S_{21}$ (coupling) between RX and TX antennas are displayed. In this simulation the spacing between the antenna and edges of the ground plane are fixed and the distance between the two antennas, $D$ is varied. As can be seen, the distance between the two antennas does not play a major role in the mutual coupling between the two antennas. This implies that the amount of coupling from surface wave propagation is not affected by the separation distance within the specified range of distances shown in Fig. 7(a). However, in choosing the ground plane size the overall dimension of the small radio repeater platform and the space for the channel isolator should be taken into account to avoid any interaction between the two antennas and the channel isolator. The optimized distance between the two antennas is found to be 25 mm. In addition, the width of the ground plane affects the level of mutual coupling due to excitation of edge currents. This effect is shown in Fig. 7(b) where all other dimensions are fixed ($D = 25$ mm, $L = 40$ mm) and $W$ is changed. To account for the integration of an RF amplifier on the backside, the dimensions of the platform are finally chosen to be 40.01 mm × 20.68 mm, which corresponds to $\lambda_0/2.75 \times \lambda_0/5.32$.

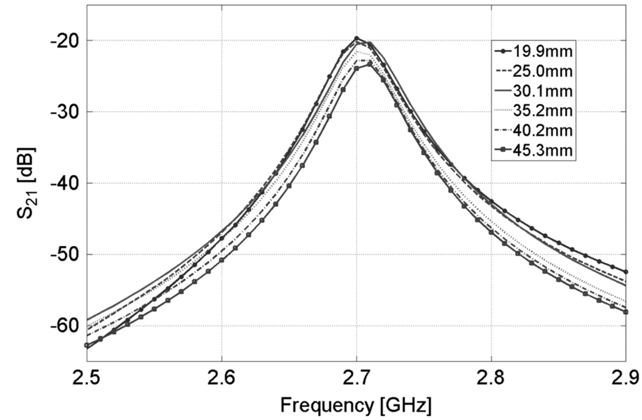


(a)

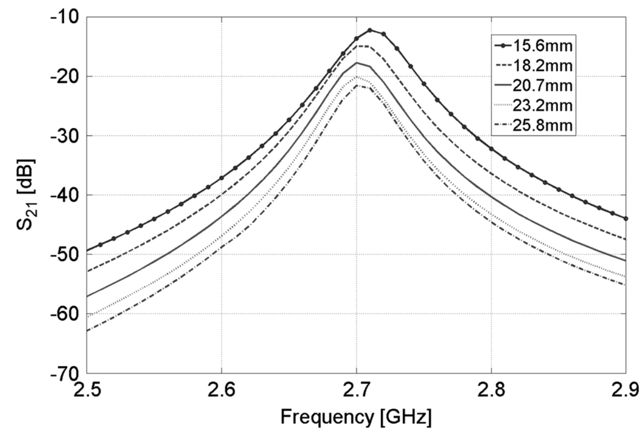


(b)

Fig. 7. Simulated coupling between antennas shown in Fig. 6: (a) varying the distance between RX and TX; (b) varying ground plane width.

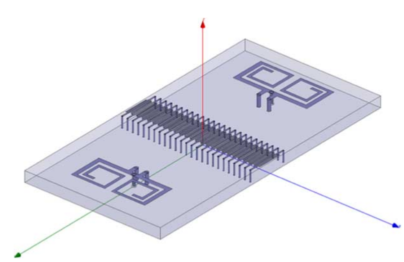

Fig. 8. Repeater platform with channel isolator.

## B. Isolator and Antenna Integration

The geometry of the proposed miniaturized radio repeater is composed of two miniaturized low-profile antennas capable of radiating vertical polarization and a metamaterial isolator layer as shown in Fig. 8. As mentioned before, close spacing between the antennas and the isolator causes the mutual coupling, and therefore it affects the performance of the repeater. Specifically, the antennas input impedances and the resonant frequency of the isolator both change as a result of the placement of the antennas and the isolator. The current distribution on the ground plane is used to evaluate the optimal placement of the isolator. As all of the physical parameters are related to each other through various electromagnetic interactions, optimization is achieved through adjusting the length of the isolator loop and the strip iteratively using HFSS.

As an initial step in the design, the RX and TX antennas as well as the isolator are designed separately. For integration, since multiple resonant structures within sub-wavelength dimensions are used, the use of manual mesh modifications in HFSS is required to capture the details of the fields around the isolator. The designed topology is in Fig. 8. Physical parameters

TABLE III
DESIGNED PARAMETERS OF THE SMALL RADIO REPEATER

| Design Parameters | Optimized Dimension |
|---|---|
| Distance between two antennas ($D$) | 24.99mm |
| Distance between two vertical wires ($l_{loop}$) | 5.84mm |
| Length of strip fingers ($l_{cap}$) | 3.38mm |
| Width of platform ($W$) | 20.68mm |
| Length of platform ($L$) | 40.01mm |
| Height of platform | 1.57mm |
| Adjusted Antenna Geometry (see Fig. 3) | Optimized Dimension |
| $l_{h4}$ | 1.21mm |
| $l_{v2}$ | 3.80mm |
| $l_{v3}$ | 3.00mm |
| $l_m$ | 0.97mm |

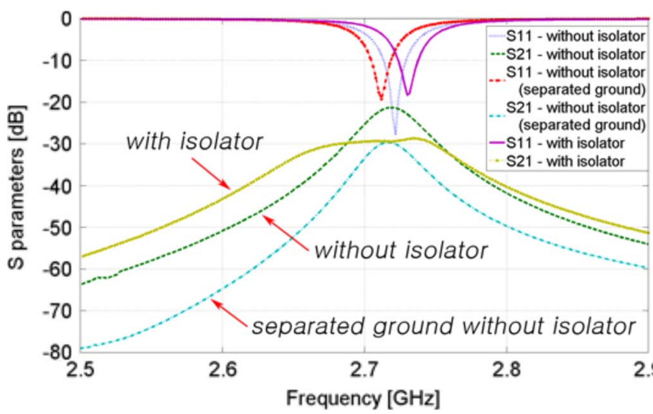


Fig. 9. Simulated S-parameters of the small radio repeater with and without the metamaterial isolator.

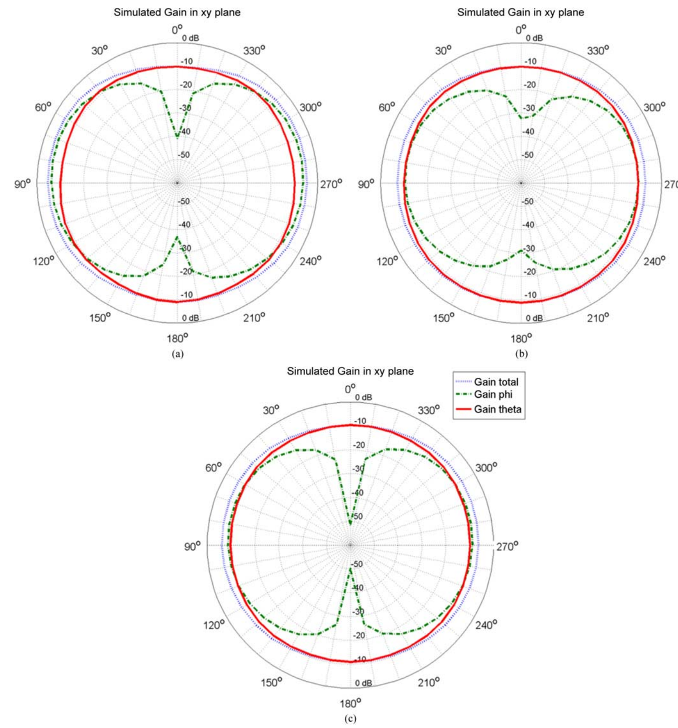


Fig. 10. Simulated radiation pattern: (a) single ground plane without isolator; (b) separated ground planes without isolator; (c) single ground plane with channel isolator.

are optimized for the repeater to operate around 2.72 GHz and are reported in Table III. The optimized simulation response and measured data are discussed in Sections IV and V.

## IV. REPEATER SIMULATION RESULTS

In this section full-wave analysis is carried out to examine the performance of the proposed repeater. Fig. 9 shows the simulated S-parameters of the optimized small radio repeater platform. As shown, a $-20$ dB of transmission coefficient can be achieved between the TX and RX antennas without the channel isolator with designed dimensions (assuming the two antennas are well matched.) Incorporating the channel isolator, the transmission coefficient drops to $-30$ dB. Also shown is that the antenna response is affected due to the interaction between the antennas and the isolator. In fact, per our design the antennas are well matched (over $-15$ dB of input reflection coefficient), and the center frequency is at the desired value in the presence of the isolator. The presence of the antenna also affects the isolator frequency response. As shown before, the resonant frequency of an isolated unit cell of the metamaterial isolator is at 2.98 GHz. With some small adjustments, in the presence of the antenna, this resonance occurs at 2.72 GHz as shown in Fig. 9.

It should be noted here that if the ground planes of transmit and receive antennas are disconnected improved isolation can be achieved. However, this way no amplifier can be inserted between the transmit and receive antennas.

The simulated radiation patterns in H plane are represented in Fig. 10. In order to provide enough area for two modified antennas and a channel isolator, the ground plane should be extended along the longitudinal direction, which breaks the symmetry of the ground plane. Although the modified MMA with square ground plane shows pure vertical polarization in H plane (see Fig. 4(d)), the horizontal induced current on the rectangular ground plane generates horizontal polarization in H plane as shown in Fig. 10(a). In all cases, however, the antenna shows around $-9$ dBi of gain in vertical polarization. The gain of the antenna is limited due to dielectric and metallic losses. Increasing the dielectric thickness and increasing antenna dimensions increase the gain. Also it should be noted that the distance between two antennas is about 25 mm. For such small separations, the coupling mainly comes from the antennas' near field.

Fig. 11 shows the magnetic field distribution over the ground plane for the repeater with and without the isolator. As expected, the horizontal magnetic field generated from the lower antenna in Fig. 11(a) propagates through the substrate and produces the mutual coupling to the top antenna. When incorporating the channel isolator, Fig. 11(b) indicates that the horizontal magnetic field is maximized within the channel isolator. This implies that the surface currents (perpendicular to the direction of magnetic field in the channel isolator) are interrupted by the isolator, as shown in Fig. 12.

## V. EXPERIMENTAL RESULTS

The prototype of the proposed small radio repeater system is fabricated using a 1.57 mm-thick Rogers RO-5880 substrate ($\epsilon_r = 2.2$), as shown in Fig. 13. Fig. 14 shows the measured S-parameters of the small radio repeater and indicates that the resonant frequency is located at 2.72 GHz. Since the fabrication process includes physical limitations such as under cutting

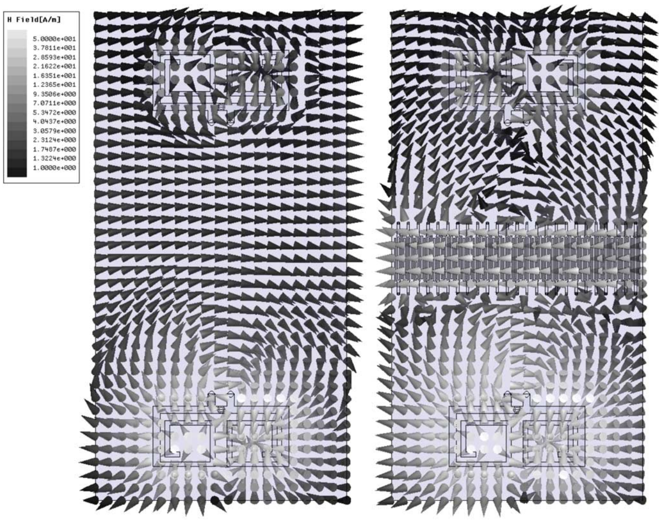

(a) (b)

Fig. 11. Simulated H field distribution: (a) small radio repeater without channel isolator; (b) small radio repeater with channel isolator.

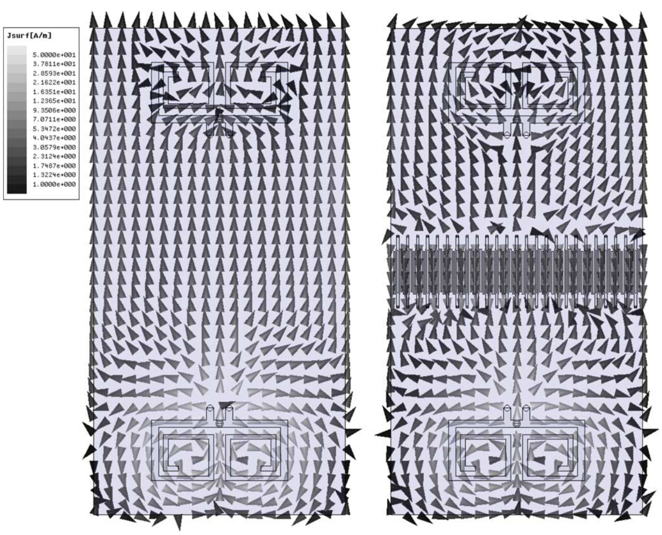

(a) (b)

Fig. 12. Simulated current distribution: (a) small radio repeater without channel isolator; (b) small radio repeater with channel isolator.

of the copper in the etching process and errors in alignment, the frequency shift between the computer based design and actual fabrication is unavoidable. However, this discrepancy can be corrected after a few trials. In addition, post tuning and optimization can be used to obtain the designed performance.

Fig. 15 shows the system setup for the measuring of S-parameters. To feed each of antennas, two microstrip transmission lines are used where one is connected to an amplifier with variable gain and its output is connected to the other antenna through a directional coupler. The directional coupler is inserted between RF amplifier and transmit antenna to monitor the occurrence of oscillation when it happens as the gain is increased. As can be seen in Fig. 14, the repeater without the channel isolator shows a $-18$ dB of transmission coefficient, and the proposed repeater shows a $-42$ dB of transmission coefficient, which indicates 24 dB of suppression improvement. With the channel

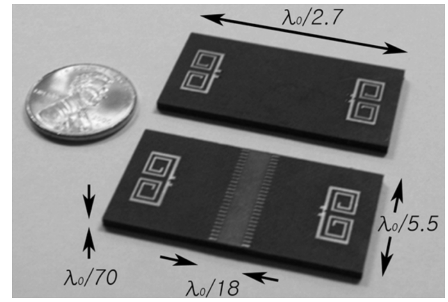


Fig. 13. Fabricated small radio repeater w/wo channel isolator.

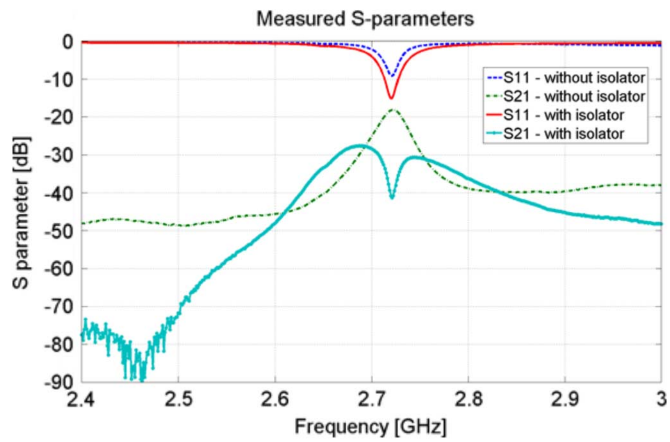


Fig. 14. Measured S-parameters of proposed small radio repeater with and without channel isolator.

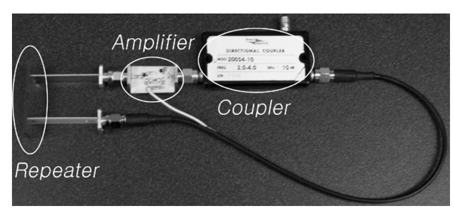


Fig. 15. Verification for operation of small radio repeater.

isolator, $-28$ dB of peak level of $S_{21}$ is observed, however, in spite of 1 dB of insertion loss from the directional coupler, a maximum gain of 32 dB for a wideband RF amplifier can be utilized with this repeater. Since the antennas are slightly mismatched near to the desired frequency (2.72 GHz), the maximum gain can be higher than the peak level of $S_{21}$. Therefore, it is verified that a commercial wideband RF amplifier with a gain of 32 dB can be integrated into the proposed repeater without oscillation.

## VI. Conclusions

In this paper, a new concept for implementation of miniaturized radio repeater is presented. To construct the radio repeater, two miniaturized low-profile antennas $(\lambda_0/70)$ radiating vertical polarization and a very thin metamaterial isolator layer are integrated into a compact configuration. The antennas are designed to have an omnidirectional radiation pattern to make the repeater insensitive to the positions of the transmitter and receiver. In addition, the proposed isolator is shown to suppress the mutual coupling, improving the transmission coefficient from $-18$ dB to $-42$ dB. The dimensions of the TX/RX antennas and a unit cell of the isolator are $11.20\ \mathrm{mm} \times 5.10\ \mathrm{mm} \times 1.57\ \mathrm{mm}$ and $5.84\ \mathrm{mm} \times 0.81\ \mathrm{mm} \times 1.57\ \mathrm{mm}$, respectively. The overall dimensions of the proposed radio repeater are $40.01\ \mathrm{mm} \times 20.68\ \mathrm{mm} \times 1.57\ \mathrm{mm}$, which corresponds to $\lambda_0/2.75 \times \lambda_0/5.32 \times \lambda_0/70$. The proposed radio repeater system has been simulated and verified experimentally. The prototype of the design has been fabricated using printed circuit technology, which serves to reduce fabrication complexity and allows for easy commercial production at a large scale.

Such a radio repeater system can mitigate the adverse effects of obstacles in radio connectivity for ad-hoc networks in complex environments.

## REFERENCES


[1] S. K. Park, P.-J. Song, and G. S. Bae, "Joint optimization of radio repeater location and linking in WLL systems with 2.3 GHz frequency band," in *Proc. IEEE Int. Conf. on Communications*, 1999, vol. 3, pp. 1617–1621.

[2] P. Slobodzian, "Estimation of the repeater gain required for a wireless link," in *Proc. 15th Int. Conf. on Microwaves, Radar and Wireless Communications*, May 2004, vol. 2, pp. 656–659.

[3] J. Borkowski, J. Niemela, T. Isotalo, P. Lahdekorpi, and J. Lempiainen, "Utilization of an indoor DAS for repeater deployment in WCDMA," in *Proc. IEEE 63rd Vehicular Technology Conf.*, May 2006, vol. 3, pp. 1112–1116.

[4] A. H. Naemat, A. Tee, A. S. M. Marzuki, B. Mohmd, K. Khalil, and A. R. A. Rahim, "Achieving optimum in-building coverage of 3 G network in Malaysia," in *Proc. IEEE Int. RF and Microwave Conf.*, Sep. 2006, pp. 343–346.

[5] B. W. Lovinggood, M. D. Judd, and W. P. Kuiper, "Integrated Repeater," U.S. Patent 6,934,511 B1, 2005.

[6] D. L. Runyon, S. B. Thompson, J. W. Maxwell, and D. L. M. SR., "Wireless Repeater With Feedback Suppression Features," U.S. Patent 2006/0 205 343 A1, 2006.

[7] T. W. Ban, B. Y. Cho, W. Choi, and H.-S. Cho, "On the capacity of a DS/CDMA system with automatic on-off switching repeaters," in *Proc. IEEE Int. Conf. on Communications*, 2001, vol. 3, pp. 780–784.

[8] M. Lee, B. Keum, Y. Son, J.-W. Kim, and H. S. Lee, "A new low-complex interference cancellation scheme for WCDMA indoor repeaters," in *Proc. IEEE Region 8 Int. Conf. on Computational Technologies in Electrical and Electronics Engineering*, Jul. 2008, pp. 457–462.

[9] D. Liao and K. Sarabandi, "Terminal-to-terminal hybrid full-wave simulation of low-profile, electrically-small, near-ground antennas," *IEEE Trans. Antennas Propag.*, vol. 56, no. 3, pp. 806–814, Mar. 2008.

[10] W. Hong and K. Sarabandi, "Low-profile, multi-element, miniaturized monopole antenna," *IEEE Trans. Antennas Propag.*, vol. 57, no. 1, pp. 72–80, Jan. 2009.

[11] D. Sievenpiper, L. Zhang, R. Broas, N. Alexopolous, and E. Yablonovitch, "High-impedance electromagnetic surfaces with a forbidden frequency band," *IEEE Microw. Theory Tech.*, vol. 47, no. 11, pp. 2059–2074, Nov. 1999.

[12] F. Yang and Y. Rahmat-Samii, "Microstrip antennas integrated with electromagnetic band-gap (EBG) structures: A low mutual coupling design for array applications," *IEEE Trans. Antennas Propag.*, vol. 51, no. 10, pp. 2936–2946, Oct. 2003.

[13] K. Buell, H. Mosallaei, and K. Sarabandi, "Metamaterial insulator enabled superdirective array," *IEEE Trans. Antennas Propag.*, vol. 55, no. 4, pp. 1074–1085, April 2007.

[14] H. Mosallaei and K. Sarabandi, "Design and modeling of patch antenna printed on magneto-dielectric embedded-circuit metasubstrate," *IEEE Trans. Antennas Propag.*, vol. 55, no. 1, pp. 45–52, Jan. 2007.

[15] R. Igreja and C. J. Dias, "Analytical evaluation of the interdigital electrodes capacitance for a multi-layered structure," *Sensors Actuat. A: Phys.*, vol. 112, no. 2–3, pp. 291–301, 2004.


**Kamal Sarabandi** (S'87–M'90–SM'92–F'00) received the B.S. degree in electrical engineering from the Sharif University of Technology, Tehran, Iran, in 1980, the M.S. degree in electrical engineering in 1986, and the M.S. degree in mathematics and the Ph.D. degree in electrical engineering from The University of Michigan at Ann Arbor, in 1989.

He is currently the Director of the Radiation Laboratory and the Rufus S. Teesdale Professor of Engineering in the Department of Electrical Engineering and Computer Science, The University of Michigan at Ann Arbor. His research areas of interest include microwave and millimeter-wave radar remote sensing, metamaterials, electromagnetic wave propagation, and antenna miniaturization. He possesses 25 years of experience with wave propagation in random media, communication channel modeling, microwave sensors, and radar systems and leads a large research group including two research scientists, 14 Ph.D. students. He has graduated 36 Ph.D. and supervised numerous post-doctoral students. He has served as the Principal Investigator on many projects sponsored by the National Aeronautics and Space Administration (NASA), Jet Propulsion Laboratory (JPL), Army Research Office (ARO), Office of Naval Research (ONR), Army Research Laboratory (ARL), National Science Foundation (NSF), Defense Advanced Research Projects Agency (DARPA), and a large number of industries. Currently he is leading the Center for Microelectronics and Sensors funded by the Army Research Laboratory under the Micro-Autonomous Systems and Technology (MAST) Collaborative Technology Alliance (CTA) program. He has published many book chapters and more than 185 papers in refereed journals on miniaturized and on-chip antennas, metamaterials, electromagnetic scattering, wireless channel modeling, random media modeling, microwave measurement techniques, radar calibration, inverse scattering problems, and microwave sensors. He has also had more than 442 papers and invited presentations in many national and international conferences and symposia on similar subjects.

Dr. Sarabandi is a member of Commissions F and D of URSI. He was the recipient of the Henry Russel Award from the Regent of The University of Michigan. In 1999, he received a GAAC Distinguished Lecturer Award from the German Federal Ministry for Education, Science, and Technology. He was also a recipient of the 1996 EECS Department Teaching Excellence Award and a 2004 College of Engineering Research Excellence Award. In 2005 he received the IEEE GRSS Distinguished Achievement Award and the University of Michigan Faculty Recognition Award. He also received the best paper Award at the 2006 Army Science Conference. In 2008 he was awarded a Humboldt Research Award from The Alexander von Humboldt Foundation of Germany and received the best paper award at the IEEE Geoscience and Remote Sensing Symposium. He was also awarded the 2010 Distinguished Faculty Achievement Award from the University of Michigan. The IEEE Board of Directors announced him as the recipient of the 2011 IEEE Judith A. Resnik medal. He served as a member of NASA Advisory Council appointed by the NASA Administrator for two consecutive terms from 2006–2010. He is serving as a Vice President of the IEEE Geoscience and Remote Sensing Society (GRSS) and is a member of the Editorial Board of the PROCEEDINGS OF THE IEEE. He was an Associate Editor of the IEEE TRANSACTIONS ON ANTENNAS AND PROPAGATION and the IEEE SENSORS JOURNAL. In the past several years, joint papers presented by his students at a number of international symposia (IEEE APS'95,'97,'00,'01,'03,'05,'06,'07; IEEE IGARSS'99,'02,'07; IEEE IMS'01, USNC URSI'04,'05,'06,'10,'11 AMTA '06, URSI GA 2008) have received best paper awards.

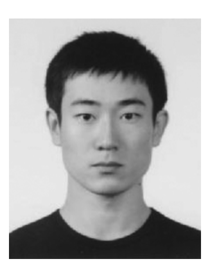

**Young Jun Song** (S'07) received the B.S. degree in electrical engineering (*summa cum laude*) from the Seoul National University, Seoul, Korea, in 2006, and the M.S. degree in electrical engineering from The University of Michigan at Ann Arbor, in 2009, where he is currently working toward the Ph.D. degree.